Efficient and Accurate Likelihood for Iterative Image Reconstruction in X-ray Computed Tomography

Idris A. Elbakri and Jeffrey A. Fessler

Electrical Engineering and Computer Science Department
University of Michigan
Ann Arbor, MI.

ABSTRACT

We report a novel approach for statistical image reconstruction in X-ray CT. Statistical image reconstruction depends on maximizing a likelihood derived from a statistical model for the measurements. Traditionally, the measurements are assumed to be statistically Poisson, but more recent work has argued that CT measurements actually follow a compound Poisson distribution due to the polyenergetic nature of the X-ray source. Unlike the Poisson distribution, compound Poisson statistics have a complicated likelihood that impedes direct use of statistical reconstruction. Using a generalization of the saddle-point integration method, we derive an approximate likelihood for use with iterative algorithms. In its most realistic form, the approximate likelihood we derive accounts for polyenergetic X-rays and Poisson light statistics in the detector scintillator, and can be extended to account for electronic additive noise. The approximate likelihood is closer to the exact likelihood than is the conventional Poisson likelihood, and carries the promise of more accurate reconstruction, especially in low X-ray dose situations.

Keywords: Statistical image reconstruction, compound Poisson distribution, log likelihood, saddle-point approximation.

1. INTRODUCTION

Accurate statistical modeling forms the foundation of statistical iterative reconstruction. The statistical model leads to a cost function that is optimized by an iterative algorithm under certain constraints. Statistical iterative reconstruction gives good bias-variance performance in nuclear medicine modalities (PET and SPECT), where counts are low and the usual Poisson data assumption works well. Recently, statistical reconstruction has gained significant inroads in X-ray computed tomography (CT). It is hoped that statistical reconstruction will overcome the limitations of the Radon transform framework, especially as non-standard scanning geometries become mainstream. The well-understood (and easy to work with!) Poisson statistical model is also frequently adopted for X-ray CT measurements. In reality, however, CT detectors are not quanta counters, and the statistics of the data are strongly dependent on the energy profile of the X-ray beam, which is usually polyenergetic.

In modern CT scanners, the X-ray source generates a polyenergetic flux of X-ray photons. The X-ray photons that are detected are converted to light photons that in turn produce photoelectrons. The current associated with these electrons is integrated and recorded digitally by an A/D channel. The number of light photons generated, and hence the recorded signal, depends on energies of the detected X-ray quanta. The energy dependence of the measurements implies that for a polyenergetic source, measurements resulting from photons at different energies will have different statistics.[1] X-ray quanta, as they individually interact with the detector, will lead to Poisson statistics, but the overall recorded signal will not be Poisson. In fact, measurements resulting from a polyenergetic source follow compound Poisson statistics.[1] Unfortunately, the log-likelihood for compound Poisson statistics is impractical for reconstruction. The focus of this paper is developing an accurate but practical approximation to the compound Poisson log-likelihood.

Send correspondence to Idris A. Elbakri
E-mail: ielbakri@umich.edu
Address: 4418 EECS Bldg, 1301 Beal Ave., Ann Arbor, MI, 48109, USA

Section 2 outlines the compound Poisson process for X-ray CT detection in terms of its characteristic function. Section 3 outlines the saddle-point approximation to integrals, which is the mathematic tool we use to approximate the likelihood. Sections 4 and 5 build on the saddle-point approximation in deriving log-likelihoods for the case of monoenergetic and polyenergetic X-rays, respectively. In Section 6 we illustrate some preliminary results. In Section 7 we discuss our results and future extensions of this work.

2. COMPOUND POISSON STATISTICS

Consider the problem of photon detection in X-ray CT from its most basic principles. Discrete photons, each at some energy W, collide with a scintillating detector, and are absorbed according to the detector quantum efficiency. The absorbed X-ray photons each generate some number of light photons. The number of incident X-ray photons is denoted by the Poisson random variable N. The number of light photons generated by each X-ray photon that is detected is also a random variable with p.m.f. $P_X(x)$. We list the random variables for the sake of clarity:

- N is the Poisson random variable with mean $\bar{N}$ that describes the number of X-ray photons that interact with the detector.

- X_n is a discrete random variable with p.m.f. $P_X(x)$ that denotes the number of light photons generated and recorded when the nth X-ray photon interacts with the scintillator. We assume that the light generation caused by an X-ray photon does not disturb subsequent generations, hence $\{X_n\}$ are i.i.d.

- Y is a discrete random variable that is proportional to the total number of recorded light photons generated by the N X-ray photons that interact with the detector.

Expressed mathematically,

$$Y \;=\; A\sum_{n=1}^{N} X_n \tag{1}$$

$$\bar{y} \;\triangleq\; E[Y] = A\bar{N}E[X], \tag{2}$$

where $E[\cdot]$ is the expectation operator and A denotes the overall efficiency of the recording system. For simplicity, we assume $A = 1$ hereafter, so Y denotes the total number of light photons recorded. Our goal is to derive a p.m.f. for Y, by deriving its moment generating function, $g_Y(z)$. Recall that the moment generating function of a discrete random variable is the Z transform of its p.m.f.

Using iterated expectations and the properties of moment generating functions,

$$\begin{aligned}
g_Y(z) \;&=\; E[z^Y] = E_N[E_Y[z^Y|N]] \\
&=\; E_N[\Pi_{n=1}^{N} E[z^X]] = E_N[E[z^X]^N] \\
&=\; \sum_{n=0}^{\infty} (g_X(z))^n P(N=n) \\
&=\; \sum_{n=0}^{\infty} (g_X(z))^n \frac{e^{-\bar{N}}\bar{N}^n}{n!} \\
&=\; \exp(-\bar{N}(1 - g_X(z))), \tag{3}
\end{aligned}$$

where $g_X(z) = E[z^X]$ is the moment generating function of X. This result is the same as that derived by Feller[2] for the moment generating function of a compound Poisson process. As a sanity check, note that

$$E[Y] = g_y'(1) = \bar{N}g_x'(1) = \bar{N}E[X].$$

Ideally, we would determine the p.m.f. $P_Y(y)$ by taking the inverse Z transform of $g_Y(z)$. However, that is often mathematically intractable. In the next section we briefly discuss saddle-point approximation and integration, which will form the basis for approximating the p.m.f in later sections.

3. SADDLE-POINT APPROXIMATION AND INTEGRATION

In this section we present a slightly generalized version of the saddle-point integration method. The saddle-point method[3] is useful for approximating some integrals that can be expressed in the exponential form

$$\frac{1}{2\pi j} \int_c e^{\Phi(z)} dz, \tag{4}$$

where z is complex and the integral is along an appropriate contour c in the complex plane. In the saddle point approximation, the exponent in the integrand is expanded in a Taylor series around a real stationary (saddle) point (assuming one exists), defined to be a root of the derivative of Φ. The first derivative term in the Taylor expansion vanishes, and the second derivative term is the highest that is retained.

More generally, we will expand the exponent around a real point that is not necessarily equal to the saddle point (but is in reality close to it). We retain the first and second derivative terms of the Taylor series. Let z_o be real in the region of convergence of the integral in (4), then we can write

$$
\begin{aligned}
\exp[\Phi(z)] &= \exp\left[\Phi(z_o) + \Phi'(z_o)(z - z_o) + \frac{1}{2}\Phi''(z_o)(z - z_o)^2 + \sum_{l=3}^{\infty} \frac{1}{l!}\Phi^{(l)}(z_o)(z - z_o)^l\right] \\
&= \exp\left[\Phi(z_o) + \Phi'(z_o)(z - z_o) + \frac{1}{2}\Phi''(z_o)(z - z_o)^2\right] f(z, z_o),
\end{aligned} \tag{5}
$$

where, based on the series expansion of the exponential function,

$$f(z, z_o) = \exp\left[\sum_{l=3}^{\infty} \Phi^{(l)}(z_o)(z - z_o)^l\right] = 1 + \frac{\Phi^{(3)}(z_o)}{6}(z - z_o)^3 + \frac{1}{2}\left(\frac{\Phi^{(3)}(z_o)}{6}(z - z_o)^3\right)^2 + O\left((z - z_o)^6\right). \tag{6}$$

The integral (4) becomes

$$\frac{1}{2\pi j}\int_c e^{\Phi(z)} dz = \frac{e^{\Phi(z_o)}}{2\pi j}\int_c e^{\Phi'(z_o)(z - z_o) + \frac{1}{2}\Phi''(z_o)(z - z_o)^2} f(z, z_o) dz. \tag{7}$$

We presume that it is acceptable to use a contour of integration that is a line that runs parallel to the imaginary axis and goes through the real point z_o. Along this contour, $z - z_o = j\omega$ where ω is the imaginary variable and the integral can be rewritten as:

$$
\begin{aligned}
\frac{1}{2\pi j}\int_c e^{\Phi(z)} dz &= e^{\Phi(z_o)} \int_{-\infty}^{\infty} e^{-\frac{1}{2}\Phi''(z_o)\omega^2} e^{j\omega\Phi'(z_o)} \left[1 + F(z_o + j\omega, z_o)\right] \frac{d\omega}{2\pi} \\
&\approx \frac{e^{\Phi(z_o) - \frac{(\Phi'(z_o))^2}{2\Phi''(z_o)}}}{\sqrt{2\pi\Phi''(z_o)}}.
\end{aligned} \tag{8}
$$

where we have used the inverse Fourier transform in the last step and assumed the integral of the remainder $[1 + F(z_o + j\omega, z_o)]$ is negligible. If z_o is an actual saddle point, then $\Phi'(z_o) = 0$ and the result reduces to the usual saddle-point approximation[3, 4]:

$$\frac{1}{2\pi j}\int_c e^{\Phi(z)} dz \approx \frac{e^{\Phi(z_o)}}{\sqrt{2\pi\Phi''(z_o)}}. \tag{9}$$

In the next section, we use the saddle point approximation (8) to derive a likelihood for the idealized case of a monoenergetic X-rays. We first briefly outline the simple case of monoenergetic X-rays with no variability in light generation in the scintillator and no electronic noise. This simplified scenario will introduce our notation and illustrate some of the more salient features of our technique.

4. MONOENERGETIC X-RAYS

We first examine the case of an X-ray source that generates a beam at a single energy. For simplicity we assume an ideal detector with no electronic noise. We examine two simple cases, with and without optical photon spread.

4.1. Monoenergetic X-ray Detection without Light Photon Statistics

Suppose there is no variability in the number of light photons recorded for each absorbed X-ray photon. The p.m.f. of the number of light photons is given by:

$$P_X(x) = \begin{cases} 1, & x = x_o \\ 0, & \text{otherwise,} \end{cases} \tag{10}$$

where x_o is the mean number of optical photons. Its value depends on the energy of the X-rays and detector design. The moment generating function for X is:

$$g_X(z) = E[z^X] = \sum_{n=0}^{\infty} z^n P_X(n) = z^{x_o}. \tag{11}$$

The moment generating function of the random variable Y is:

$$g_Y(z) = \exp(-\bar{N}(1 - z^{x_o})). \tag{12}$$

As a sanity check, when $x_o = 1$ (i.e., we have an X-ray photon counting detector), $g_Y(z)$ is reduces to the regular Poisson generating function $\exp(-\bar{N}(1 - z))$. Alternatively, the generating function of the Poisson random variable $Y' = \frac{Y}{x_o}$ is $g_Y(z^{\frac{1}{x_o}})$ which is also the simple Poisson generating function.

To find the p.m.f. of Y, we using the contour integral form of the inverse Z transform to invert $g_Y(z)$:

$$\begin{aligned} P_Y(y) &= \frac{1}{2\pi j} \int_c z^{-y-1} g_Y(z) dz \\ &= \frac{1}{2\pi j} \int_c z^{-y-1} e^{-\bar{N} + \bar{N} z^{x_o}} dz = \frac{1}{2\pi j} \int_c e^{\Phi_y(z)} dz, \end{aligned}$$

where

$$\Phi_y(z) = -(y+1)\log z - \bar{N} + \bar{N} z^{x_o}.$$

Although the Z transform can in this case be inverted by inspection, for illustration we use the saddle point approximation method.[3–5] The saddle point z_o of $\Phi_y(z)$ is the real root of

$$\Phi_y'(z) = -\frac{(y+1)}{z} + \bar{N} x_o z^{x_o-1} = 0. \tag{13}$$

The saddle point is easily seen to be:

$$z_o(y) = \left(\frac{y+1}{\bar{N} x_o}\right)^{\frac{1}{x_o}} = \left(\frac{y+1}{\bar{y}}\right)^{\frac{1}{x_o}}, \tag{14}$$

since $\bar{y} = \bar{N} x_o$. Evaluating Φ_y and Φ_y'' at the saddle point yields

$$\begin{aligned} \Phi_y(z_o) &= \frac{(y+1)}{x_o} \log \frac{x_o \bar{N}}{(y+1)} - \bar{N} + \frac{(y+1)}{x_o} \\ \Phi_y''(z_o) &= -\frac{1}{2} \log(y+1) x_o - \frac{1}{x_o} \log \frac{x_o \bar{N}}{(y+1)}. \end{aligned}$$

Taking the log of the saddle point approximation (9) to the p.m.f. gives the likelihood:

$$\log P_Y(y) \equiv \frac{1}{x_o} \left[y \log \bar{y} - \bar{y} \right], \tag{15}$$

where constant terms are dropped. This saddle-point approximation of the log likelihood is equivalent to the conventional Poisson log likelihood, which gives some reassurance of the utility of this method.

In image reconstruction, we want to maximize the log likelihood over the set of solutions in object space. The dependence on the object comes from the fact that the mean number of X-ray photons, $\bar{N}$, depends on the object attenuation. In the monoenergetic problem,

$$\bar{N} = N_o \exp\left(- \int_{\text{Ł}} \mu(x, w_o) dl \right)$$

where the integral in the exponent is a line integral over the ray Ł. If we let $t = \int_{\text{Ł}} \mu(x, w_o) dl$ denote the line integral, then the likelihood (15) has the usual form:

$$L_y(t) \equiv \frac{y}{x_o} \log e^{-t} - N_o e^{-t}. \tag{16}$$

The result of the simple case will be useful throughout this paper. We next discuss an important generalization, where light generation is variable, as it is in practice.

4.2. Monoenergetic X-ray Detection with Poisson Light Statistics

In the above derivation, we have ignored the statistics of the light photons generated by the scintillation process. Light generation in scintillating phosphor is a very complex process. Detected X-ray photons can generate a number of charge carriers that can generate light, or scatter and generate secondary carries that in turn can also produce light. An absorbed X-ray photon can generate a burst of light, which in turn will undergo a complex diffusion process, characterized by hundreds of scattering incidents per light photon.[6] K-edge effects can also have a strong impact on the amount of light generated.[7]

As a first approximation, we assume that a detected X-ray photon will generate a Poisson number of light photons with mean number proportional to the X-ray energy, and derive an approximate likelihood based on monoenergetic X-rays. For this assumption, the Poisson p.m.f. P_X is:

$$P_X(x) = \frac{x_o^x e^{-x_o}}{x!}, \tag{17}$$

where x represents the number of light photons generated by one of the N detected X-ray photons, and $x_o = G w_o$ is the mean number of light photons and G is a scaling constant that is characteristic of the scintillating phosphor and detector design. The moment generating function of this Poisson distribution is

$$g_X(z) = \exp\left[x_o(z - 1) \right]. \tag{18}$$

Substituting into (3), we get the moment generating function of the measured signal Y

$$g_Y(z) = \exp\left[-\bar{N}(1 - e^{-x_o(1-z)}) \right], \tag{19}$$

and the associated p.m.f. is

$$P_Y(y) = \frac{1}{2\pi j} \int_c z^{-y-1} g_Y(z) dz = \frac{1}{2\pi j} \int_c e^{\Phi_y(z)} dz, \tag{20}$$

where

$$\begin{aligned}
\Phi_y(z) &= -(y+1) \log z - \bar{N} + \bar{N} e^{-x_o(1-z)} \\
\Phi_y'(z) &= -\frac{(y+1)}{z} - \bar{N} x_o e^{-x_o(1-z)} \\
\Phi_y''(z) &= \frac{(y+1)}{z^2} + \bar{N} x_o^2 e^{-x_o(1-z)}.
\end{aligned}$$

A saddle point is not available analytically from $\Phi'_y(z) = 0$. It is possible to compute the saddle point numerically, but that approach would be computationally prohibitive in the context of iterative image reconstruction, where the saddle point needs to be updated at every iteration.

Rather than use the exact saddle point, we use the saddle point derived for the monoenergetic source (without accounting for optical blur) with the generalized saddle point integration approximation discussed in Section 3. From (14), the monoenergetic case saddle point is simply

$$z_o(y) = \left(\frac{y+1}{\bar{N}x_o}\right)^{\frac{1}{x_o}}. \tag{21}$$

Evaluating Φ_y and its first two derivatives at this z_o gives:

$$\Phi_y(z_o) = -\frac{y+1}{x_o}\log\frac{(y+1)}{\bar{N}x_o} - \bar{N} + \bar{N}e^{-x_o(1-z_o(y))} \tag{22}$$

$$\Phi'_y(z_o) = -(y+1)\left(\frac{\bar{N}x_o}{y+1}\right)^{\frac{1}{x_o}} + \bar{N}x_o e^{-x_o(1-z_o(y))} \tag{23}$$

$$\Phi''_y(z_o) = (y+1)\left(\frac{y+1}{\bar{N}x_o}\right)^{-\frac{2}{x_o}} + \bar{N}x_o^2 e^{-x_o(1-z_o(y))}. \tag{24}$$

It is now possible to write the approximate likelihood by plugging (22)-(24) in (8).

Note that x_o is the mean number of light photons, which is usually in the range of hundreds to thousands.[6, 7] Assuming the x_o is large enables us to make the following approximations:

$$e^{-x_o(1-z_o)} = \exp\left[-x_o\left(1 - \left(\frac{y+1}{\bar{N}x_o}\right)^{\frac{1}{x_o}}\right)\right] \approx \left(\frac{y+1}{\bar{N}x_o}\right)$$

$$\left(\frac{y+1}{\bar{N}x_o}\right)^{\frac{1}{x_o}} \approx 1,$$

which simplify Φ_y and its derivatives to

$$\Phi_y(z_o) \approx \frac{y}{x_o}\log\frac{\bar{N}x_o}{y} - \bar{N}$$

$$\Phi'_y(z_o) \approx 0$$

$$\Phi''_y(z_o) \approx (y+1)(1+x_o). \tag{25}$$

Under these approximations, the first derivative is zero and the second derivative is a constant. The log likelihood is equal to $\Phi_y(z_o)$. The large optical gain approximation essentially leads to the same result as the earlier section where the likelihood was derived without optical spread. Also note that this result is equivalent to the Poisson likelihood of the variable Y/x_o. This again serves as a sanity check, since large optical generation does in reality lead to Poisson-like statistics. Another reassurance comes from (19). If x_o is large, $g_{\frac{Y}{x_o}}(z) = g_Y(z^{\frac{1}{x_o}}) \approx \exp[-\bar{N}(1-z)]$ which is the Poisson moment generating function. These results also justify using the Poisson likelihood for monoenergetic CT. Polyenergetic CT, however, is more complex, and is the subject of the next section.

5. POLYENERGETIC CT

Clinical X-ray CT sources are truly polyenergetic, producing a continuum of energies. It is possible to generalize the likelihood and the saddle point approximation to the continuous X-ray spectrum case. However, when it comes to practical implementation, the continuous spectrum is represented by a discrete sum. We will use

such a discrete approximation to the continuous spectrum as our starting point for deriving an approximate likelihood.

Let the X-ray source produce photons at L distinct energies $\{w_l\}_{l=1}^L$. The p.m.f. of the X-ray beam incident on the object is:

$$P_W(w) = \sum_{l=1}^L p_l \cdot 1_{\{w=w_l\}}, \quad \sum_{l=1}^L p_l = 1,$$

where $1_{\{w=w_l\}}$ is the indicator function for the X-ray energies. The X-ray beam traverses the object and experiences energy-dependent attenuation. The amount of attenuation is exponentially related to the path that the X-ray beam takes through the object, as expressed mathematically by the line integral. For simplicity here, we adopt the following attenuation model:

$$\mu(x; w) = m(w)\rho(x), \tag{26}$$

where $m(w)$ is the mass attenuation coefficient of tissue and $\rho(x)$ is the tissue density. This model can be generalized to allow multiple tissue components.[8] We use this model because it separates the energy and spatial components of the attenuation coefficient. This model gives the following expression for the line integral:

$$\int_{\text{L}} \mu(x; w)dl \; = \; m(w) \int_{\text{L}} \rho(x)dl \tag{27}$$

$$= \; m(w)\, s. \tag{28}$$

The energy p.m.f. of the attenuated X-ray beam is:

$$\tilde{p}_W(w|s) = \sum_{l=1}^L \tilde{p}_l(s) \cdot 1_{\{w=w_l\}} \tag{29}$$

where

$$\tilde{p}_l(s) = \frac{p_l e^{-m(w)\,s}}{\sum_{k=1}^L p_k e^{-m(w_k)\,s}}. \tag{30}$$

The denominator is a normalizing factor that ensures that the p.m.f. sums to one. The number of photons interacting with the detector is the Poisson random variable N with mean

$$\bar{N}(s) = N_o \sum_{l=1}^L p_l e^{-m(w_l)s} \tag{31}$$

where N_o is the total number of photons emitted by the X-ray source.

The next step in modeling CT measurements is to add to the polyenergetic physics and compound Poisson statistics the non-trivial statistical distribution for light photons generated in the scintillator. We again assume that individual X-ray quanta generate Poisson light with mean proportional to the generating X-ray energy. In other words, the conditional light p.m.f. is

$$P_X(x|w) = \frac{(Gw)^x e^{-Gw}}{x!}. \tag{32}$$

The non-conditional p.m.f. $P_X(x; s)$ is given by

$$P_X(x; s) = \sum_{l=1}^L \tilde{p}_l(s)\frac{(x_l)^x e^{-x_l}}{x!}, \tag{33}$$

where $x_l = E[x|w = w_l] = Gw_l$ is the mean number of light photons generated by an absorbed X-ray photon with energy w_l. This p.m.f. represents a Poisson distribution at each energy/optical gain value x_l weighted by $\tilde{p}_l$ such that the overall sum adds to unity. The moment generating function exhibits the same weighting:

$$
\begin{aligned}
g_X(z;s) &= \sum_{n=0}^{\infty} \sum_{l=1}^{L} z^n \tilde{p}_l(s) \frac{(x_l)^x e^{-x_l}}{x!} \\
&= \sum_{l=1}^{L} \tilde{p}_l(s) e^{x_l(z-1)}.
\end{aligned}
\tag{34}
$$

The compound Poisson moment generating function of the total number of recorded light photons Y is

$$
g_Y(z;s) = \exp\left[-\bar{N}(s)\left(1 - \sum_{l=1}^{L} \tilde{p}_l(s) e^{x_l(z-1)}\right)\right].
\tag{35}
$$

As before, the probability density function of Y is given by

$$
P_Y(y;s) = \frac{1}{2\pi j} \int_c z^{-y-1} g_Y(z) dz,
\tag{36}
$$

where

$$
\Phi_y(z) = -(y+1)\log z - \bar{N}(s) + \bar{N}(s) \sum_{l=1}^{L} \tilde{p}_l(s) e^{-x_l(1-z)}
\tag{37}
$$

$$
\Phi_y'(z) = -\frac{(y+1)}{z} - \bar{N}(s) \sum_{l=1}^{L} \tilde{p}_l(s) x_l e^{-x_l(1-z)}
\tag{38}
$$

$$
\Phi_y''(z) = \frac{(y+1)}{z^2} + \bar{N}(s) \sum_{l=1}^{L} \tilde{p}_l(s) x_l^2 e^{-x_l(1-z)}.
\tag{39}
$$

Note that the results are very analogous to the monoenergetic case. We pursue the analogy and evaluate Φ_y and its derivatives at a saddle point estimate similar to (14), since an analytic saddle point is not available,

$$
\hat{z}_o(y;s) = \left(\frac{y+1}{\bar{N}(s)\bar{x}(s)}\right)^{\frac{1}{\bar{x}(s)}},
\tag{40}
$$

where $\bar{x}(s) \triangleq \sum_{l=1}^{L} \tilde{p}_l(s) x_l$ is the effective mean number of light photons. We take the approximation one step further. Often an iterative algorithm is initialized with a good starting image whose line integrals are computed, compared to the data, and then the image is updated. It is reasonable to assume that, with a good starting image, successive updates of s will not affect $\bar{x}(s)$ much. We therefore assume there exists an estimate $\hat{s}$ of s (from a good initial image) and use the following approximation to the saddle point,

$$
\hat{z}_o(y;s) = \left(\frac{y+1}{\bar{N}(s)\hat{x}}\right)^{\frac{1}{\hat{x}}},
\tag{41}
$$

where $\hat{x} = \bar{x}(\hat{s})$. Since $\hat{x}$ is likely to be in the range of hundreds to thousands, we can use the large optical gain approximation, which, for large $\hat{x}$, gives,

$$
e^{-x_l(1-\hat{z}_o)} = \exp\left[-x_l\left(1 - \left(\frac{y+1}{\bar{N}\hat{x}}\right)^{\frac{1}{\hat{x}}}\right)\right] \approx \left(\frac{y+1}{\bar{N}\hat{x}}\right)^{\frac{x_l}{\hat{x}}}.
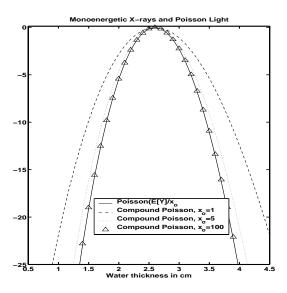\tag{42}
$$

Figure 1. Plots of the monoenergetic compound Poisson and regular Poisson likelihood. As the mean number of light photons increases, the compound Poisson likelihood approaches the regular Poisson.

This approximation simplifies Φ_y and its derivatives, resulting in the following approximate polyenergetic CT (compound Poisson) likelihood:

$$L(y;s) \approx \frac{y}{\hat{x}} \log \bar{N}(s)\hat{x} - \bar{N}(s) + \bar{N}(s) \sum_{l=1}^{L} \tilde{p}_l(s) \left(\frac{y+1}{\bar{N}\hat{x}}\right)^{\frac{x_l}{\hat{x}}} - \frac{1}{2} \frac{\left(\bar{N}(s) \sum_{l=1}^{L} \tilde{p}_l(s)x_l \left(\frac{y+1}{\bar{N}\hat{x}}\right)^{\frac{x_l}{\hat{x}}} - (y+1)\left(\frac{y+1}{\bar{N}\hat{x}}\right)^{-\frac{1}{\hat{x}}}\right)^2}{\left((y+1)\left(\frac{y+1}{\bar{N}\hat{x}}\right)^{-\frac{2}{\hat{x}}} + \bar{N}(s) \sum_{l=1}^{L} \tilde{p}_l(s)x_l^2 \left(\frac{y+1}{\bar{N}\hat{x}}\right)^{\frac{x_l}{\hat{x}}}\right)}.$$

$$(43)$$

As the optical mean becomes larger, the last term approaches a constant with respect to s, and may be dropped.

To summarize, we have derived a likelihood approximation based on the compound Poisson statistics of X-ray CT detectors, assuming that light photons generated in the scintillator material follow the Poisson distribution with mean proportional to the X-ray energy. In the next section we will present some plots of this likelihood for high and low incident CT flux, and compare with plots for the regular Poisson likelihood, which is often used for CT iterative reconstruction, and plots for a numerically computed exact likelihood.

6. PRELIMINARY RESULTS

To evaluate the proposed likelihood, we compare it to a numerically computed exact likelihood and the regular Poisson likelihood.

First we verify the large optical gain approximation. In Fig. 1 we compare the monoenergetic compound Poisson likelihood with different values of x_o to the Poisson likelihood of the random variable Y/x_o. These likelihood are generated with an initial X-ray photon count of 1000, propagating through water ($\mu = 0.23$ cm^{-1}). The water thickness is the independent variable in the figure. The exact likelihood is plotted with mean number of light photons equal to 1, 5 and 100. It can be readily seen that as the mean number of light photons increases, the compound Poisson likelihood approaches a regular Poisson likelihood, as predicted earlier.

To verify the accuracy of our method in the polyenergetic case, we compare the proposed likelihood to a numerically computed exact likelihood. Computing the exact likelihood is computationally expensive, and we
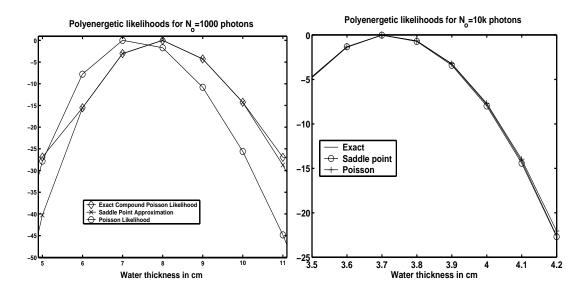
Figure 2. Plots of the polyenergetic compound Poisson, regular Poisson and exact likelihoods for an x-ray flux of 1000 photons and 10000 photons incident on water.

herein present the results for only two signal levels ($N_o = 1000$ and $N_o = 10000$ incident photons) in Fig. 2. These likelihoods were generated using an 80 kVp spectrum incident on water, with $G = 10$ photons per keV and $\hat{x} = 572$ photons. Both figures show good agreement between the proposed and exact likelihoods. For the higher photon flux case, the regular Poisson likelihood agrees very well with the exact likelihood also.

To further assess the proposed method in a situation more similar to those encountered in image reconstruction, we compute the polyenergetic likelihoods that are actually the sums of several other likelihoods. Because the measurements are statistically independent, the log likelihoods add. Fig. 3 schematically illustrates this numerical experiment. We compute compound Poisson likelihoods for the signals "recorded" by each individual detector and then sum the likelihoods. The complexity of this scenario is increased by having each detector "see" a different measurement mean, resulting in individual likelihoods with different extrema. Fig. 4 illustrates the individual likelihoods and their likelihood sum for the case of $N_o = 1$ million photons. We use the 80 kVp spectrum with $\hat{x} = 572$. For simplicity in this case, we use five different constant values for the attenuation coefficients between 0.1 cm^{-1} and 0.5 cm^{-1}. In reality the attenuation coefficients also vary with energy.

Fig. 5 illustrates the cumulative likelihoods for low ($N_o = 1000$) and high ($N_o = 1$ million) X-ray photons. The regular Poisson likelihoods (with mean $\bar{N}(s)x(s)$) are also plotted for comparison. The Poisson likelihoods are scaled by $\hat{x}$. The saddle-point approximate likelihood and the regular Poisson likelihood reach their respective maxima at different points in the low and high signal level cases. Given the simplicity of the scenario, this is an encouraging result. The higher accuracy of the proposed likelihood suggests that iterative reconstruction based on regular Poisson statistics may not lead to the optimal solution.

7. DISCUSSION

The major contribution of this work has been to derive an approximation to the log likelihood of the CT reconstruction problem, based on the more accurate compound Poisson statistical distribution and polyenergetic physics. Preliminary results show that the proposed likelihood is more accurate than the regular Poisson likelihood, especially in situations of low counts. For the simplistic scenarios examined, the discrepancy between the proposed and regular Poisson likelihoods is not very large, but may not be insignificant in the context of image reconstruction quality. Further examination of more realistic situations is necessary to ascertain the full utility of developing iterative reconstruction algorithms based on compound Poisson statistics.
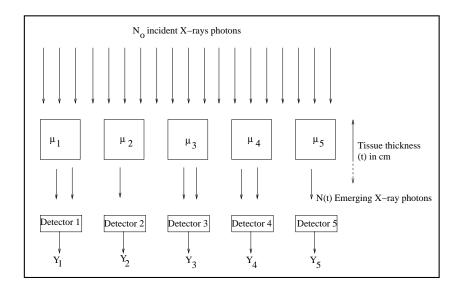
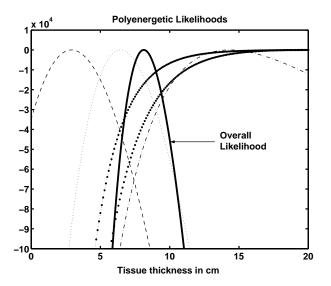**Figure 3**. Schematic of scenario used to compute cumulative polyenergetic likelihood.

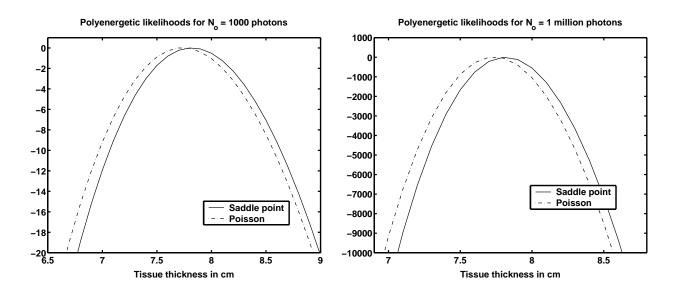**Figure 4**. Plots of individual likelihoods and the overall likelihood resulting from their sum.

Figure 5. Plots illustrating the cumulative polyenergetic compound Poisson and regular Poisson likelihoods for the schematic shown in Fig. 3 with incident x-ray flux of 1000 photons and 1 million photons.

The proposed likelihood may prove useful once the model and resulting likelihoods incorporate additive electronic noise. This anticipated result could have positive implications for reconstruction from CT measurements obtained with detectors with high electronic noise, such as CCD cameras. Future work will also include developing iterative algorithms based on the proposed likelihoods and comparing them with algorithms based on the Poisson distribution. Statistical iterative reconstruction with the compound Poisson likelihood may lead to the practical advantage of lowering X-ray dose with little sacrifice in image quality.

ACKNOWLEDGMENTS

REFERENCES

1. B. R. Whiting, "Signal statistics in x-ray computed tomography," in *Proc. SPIE 4682, Medical Imaging 2002: Med. Phys.*, 2002.
2. W. Feller, *An Introduction to Probability Theory and Its Applications*, Wiley, New York, 1968. p. 190, 245.
3. C. Helstrom, "Approximate evaluation of detection probabilities in radar and optical communications," *IEEE Tr. Aero. Elec. Sys.* **14**, pp. 630–40, July 1978.
4. M. Yavuz and J. A. Fessler, "Statistical image reconstruction methods for randoms-precorrected PET scans," *Med. Im. Anal.* **2**(4), pp. 369–378, 1998.
5. D. L. Snyder, C. W. Helstrom, A. D. Lanterman, M. Faisal, and R. L. White, "Compensation for read-out noise in CCD images," *J. Opt. Soc. Am. A.* **12**, pp. 273–83, February 1995.
6. J. Beutel, H. L. Kundel, and R. L. V. Metter, eds., *Handbook of Medical Imaging, Volume 1*, SPIE Press, Bellingham, 2000.
7. A. Ginzburg and C. E. Dick, "Image information transfer properties of x-ray intensifying screens in the energy range form 17 to 320 KeV," *Med. Phys.* **20**, pp. 1013–1021, July 1993.
8. I. Elbakri and J. A. Fessler, "Statistical image reconstruction for polyenergetic X-ray computed tomography," *IEEE Tr. Med. Im.* **21**, pp. 89–99, Feb. 2002.